Journal of Magnetism and Magnetic Materials 476 (2019) 18–23

Contents lists available at ScienceDirect

Journal of Magnetism and Magnetic Materials

journal homepage: www.elsevier.com/locate/jmmm

Research articles

Enhancement in magnetic and dielectric properties of the ruthenium-doped copper ferrite($Ru - CuFe_2O_4$) nanoparticles

V. Manikandan[a,*], V. Kuncser[b], Bogdan Vasile[c], S. Kavita[d], S. Vigneselvan[e], R.S. Mane[f]

[a] Department of Physics, Kongunadu Arts and Science College, Coimbatore 641 029, India
[b] National Institute of Materials Physics, Laboratory of Magnetism and Superconductivity, 405A Atomistilor Str., RO-77125 Magurele, Romania
[c] University Politehnica of Bucharest, Gh. Polizu Street No.1-7, 011061 Bucharest, Romania
[d] Centre for Automotive Energy Materials, International Advanced Research Centre for Powder Metallurgy and New Materials, Chennai, Tamil Nadu 113, India
[e] Department of Physics, Government College of Technology, Coimbatore 641013, India
[f] Center for Nanomaterial & Energy Devices, Swami Ramanand Teerth Marathwada University, Dnyanteerth, Vishnupuri, Nanded 431606, India

ARTICLE INFO

Keywords:
Ferrites
Dielectric properties
Soft magnetic nature
Copper ferrite
Microstructure

ABSTRACT

Ruthenium-doped copper ferrite($Ru - CuFe_2O_4$)nanoparticles (NPs) have been synthesized using a simple and cost-effective wet chemical co-precipitation deposition method. The crystallographic scanning electron microscopy images confirm cubic crystal structure and agglomerated-type surface appearance. The crystallite sizes are 6–24 nm in the range. Dielectric measurement analysis estimates the dielectric constant and loss of $Ru - CuFe_2O_4$ NPs. In this connection, dielectric constant and loss are reduced virtue of air annealing for various temperatures. Also, the dielectric loss confirms the relaxation peak. From magnetic measurement results, the coercivity decreases whereas saturation and remanence magnetization are increased. These features have approved the soft magnetic nature in the $Ru - CuFe_2O_4$ NPs.

1. Introduction

In recent time, ferrite materials have endowed their merits in the magnetic resonance imaging, drug delivery, data storage and medical oriented technology applications greatly. In the medical field, the ferrite nanoparticles (NPs) manufactured in the form of capsules can be transferred into a human body to target the cancer cells in presence of the magnetic field [1,2]. They are in the form of soft or hard magnets and are basically temperature dependent. Copper ferrite ($CuFe_2O_4$) attained a majority of concerns in solid state physics, mineralogy, ceramics and metallurgy [3]. By virtue of the phase transition and semiconducting character, the $CuFe_2O_4$ is one of the upper class emerging materials among spinel ferrites family [4,5]. Usually, $CuFe_2O_4$ has two crystallographic spinel structures; high temperature cubic phase followed low temperature tetragonal phase. An ideal inverse configuration of the $CuFe_2O_4$ consists of eight divalent ions placed at octahedral sub-lattice sites and sixteen trivalent ions situated at octahedral and tetrahedral sub-lattice sites [6]. Total magnetic moment of the $CuFe_2O_4$ depends upon uncompensated magnetic moments of eight divalent copper ions located at octahedral sub-lattice sites. The magnetic moment per unit cell i.e. $\mu = 8*1\mu_B = 8\mu_B$, for each copper ions is assumed to be 1 μ_B, where μ_B is the Bohr magnetron, which is responsible for a small energy difference among the copper ions found at octahedral and tetrahedral sites [7]. Here, cation redistribution, a function of annealing temperature can be favored. Compared with the tetragonal crystal structure, cubic crystallographic phase of the $CuFe_2O_4$ results a large magnetic moment [8], enabling researchers to look after into a desired magnetic and dielectric properties in presence of either dopant or substitutional elements. The dielectric constant and loss are crucial quantities while designing the microelectronic devices. In general, ferrites are temperature and frequency dependent and also confirm the sensitivity towards the synthesis methods used [9]. In the last two decades, the dielectric properties of ferrites have been investigated vigorously, but investigations on the rare earth metal-doped ferrites have not been yet addressed completely. The relaxation behavior of ferrites is influenced by the crystal structure and the surface morphology. The dielectric loss is useful for insulation and isolation required in microelectronic circuits. The ferromagnetic $CuFe_2O_4$ holds a wide range of applications owing to its thermal stability [10,11] and electromagnetism which also can be attained on the addition of impurities or dopants [12]. The cation redistribution of copper ferrite using substitution, usually, alters the magnetic and electric properties [13] which are size dependent [14,15]. Trivalent, highly catalytic and electrically active ruthenium (Ru) was considered as dopant in the

* Corresponding author.
E-mail address: manikandan570@gmail.com (V. Manikandan).

https://doi.org/10.1016/j.jmmm.2018.12.050
Received 1 August 2018; Received in revised form 10 November 2018; Accepted 11 December 2018
Available online 11 December 2018

present work for knowing changes in the magnetic and dielectric properties of $CuFe_2O_4$. Satter et al. reported the use of rare earth metal oxide-doped Cu-Zn ferrites for obtaining an enhanced effective magnetic moment at the cost of resultant magnetization [16]. Ghasemi et al. presented a soft magnetic behavior of the Dy^{3+}-substituted Ni-Cu-Zn ferrite NPs with increased saturation magnetization as a function of exchange interaction among Fe-Fe ions and also the particle size [17]. The purpose of the Ru-doping was to enhance the soft magnetic nature in addition to dielectric properties which can be beneficial in the magnetic tape recording as doping of the trivalent rare earth elements offers a better magnetic performance [18]. To the best of our knowledge, electrical and magnetic properties of the Ru-doped $CuFe_2O_4$ i.e., $Ru-CuFe_2O_4$ NPs have not so far reported in the literature. Here, we report the use of eco-friendly and economic wet chemical co-precipitation chemical method for synthesis of $Ru-CuFe_2O_4$NPsand their dielectric and magnetic properties to achieve an enhanced soft magnetism.

2. Experimental method

The$Ru_xCuFe_{2-x}O_4$(x = 0.02)NPs were synthesized from $RuCl_3$. $2H_2O$, $CuCl_2$. $6H_2O$, $FeCl_3$. $9H_2O$ by a wet co-precipitation chemical method. Starting chemicals were dissolved into the double distilled water while continuous stirring at 2 h. With the effect of stirring, the precursor solution showed a light green color. On pouring sodium hydroxide solution the precursor solution turned into a dark brown which was cleaned using double distilled water for several times to remove the impurities, if there are any, which was then dried at hot air-oven, and maintained in day/night at 150 °C for 6 h. The mud-like precipitate was completely dried and then transferred into a mortar agate for manually grinding process before getting a fine powder. This powder was inserted into a silica crucible which was placed in muffle-furnace for annealing process which was maintained at 300, 600 and 900 °C for 5 h before measuring the physical, electrical, magnetic and dielectric properties.

2.1. Characterizations

As-obtained $Ru-CuFe_2O_4$ NPs were scanned for X-ray diffractometer (Model ULTIMA III) for the structural elucidation. An information on the surface evolution details was obtained from the scanning and transmission electron microscopy images recorded on the SEM JEOL 5600V) and JEOLJEM 2100HR units. Surface elementals were evidenced from the energy dispersive X-ray spectroscopy (EDX) measurement, associated with TEM unit. Dielectric properties of $Ru-CuFe_2O_4$ NPs were demonstrated using LCR meter (HIKOI 3532-50 LCR) and for knowing the soft magnetic nature vibrational magnetometer (Microsense Inc. USA (EZ9 model) was used.

3. Results and discussion

3.1. Structural analysis

Fig. 1 presents the XRD patterns of $Ru-CuFe_2O_4$NPs obtained on air-annealing at 300, 600 and 900 °C annealing temperatures for 5 h. From these figure, the indexed reflection peaks are consistent to the JCPDS card (77-0010). Also, the Fd3m space group was present [19] and also $Ru-CuFe_2O_4$demonstrated secondary phase (Fe_2O_3) owing to iron vacancy in sub-lattices which is annealing temperature dependent [20]. Due to annealing temperature, an elevated intensity peaks in the XRD spectra ensured an enhanced crystallinity with increase in the crystallite size from 6 to 24 nm. Particle sizes were obtained from the

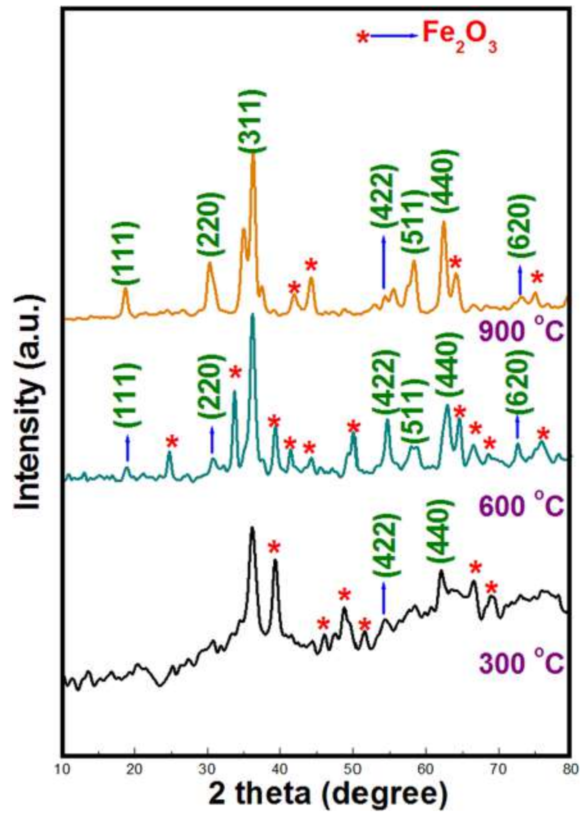

Fig. 1. XRD patterns of $Ru-CuFe_2O_4$NPs annealed at 300, 600 and 900 °C temperatures.

(3 1 1) reflection plane which confirms the formation $Ru-CuFe_2O_4$ NPs [21].

3.2. Microstructure confirmation and elemental analysis

Fig. 2(a-b) highlights the SEM images of 900 °C annealed $Ru-CuFe_2O_4$ NPs at two different magnifications where the formation of cubic crystallites is clearly evidenced. Also, annealed $Ru-CuFe_2O_4$NPs showed well-defined polished cuboids. Fig. 2(c-d) presents the microstructure and selected-area electron diffraction pattern images of the $Ru-CuFe_2O_4$ NPs. Cubic crystallites as seen in Fig. 2c were consistent to SEM analysis. From Fig. 2c, the NPs of $Ru-CuFe_2O_4$ were slightly agglomerated, which is unavoidable in most of the ferrites. Fig. 2d reveals bright spots in addition to circular rings, suggesting nanocrystallinity involvement rather than polycrystallinity and single crystallinity [22]. Fig. 2e shows the surface chemical composition where, existence of elements in various proportions like O, Fe, Cu, Ru was confirmed, revealing formation of $Ru-CuFe_2O_4$.

3.3. Dielectric properties

Fig. 3 depicts changes in the dielectric constants of the$Ru-CuFe_2O_4$ NPs recorded under various annealing temperatures. Dielectric behavior of $Ru-CuFe_2O_4$NPs was scanned between 1 and 7 log frequency range (Hz) at ambient temperature [23]. Further, decrease in the dielectric constant of the $Ru-CuFe_2O_4$ NPs with frequency was attributed to a dielectric dispersion [24]. At low frequency, the decrease of dielectric constant was rapid whereas high frequency

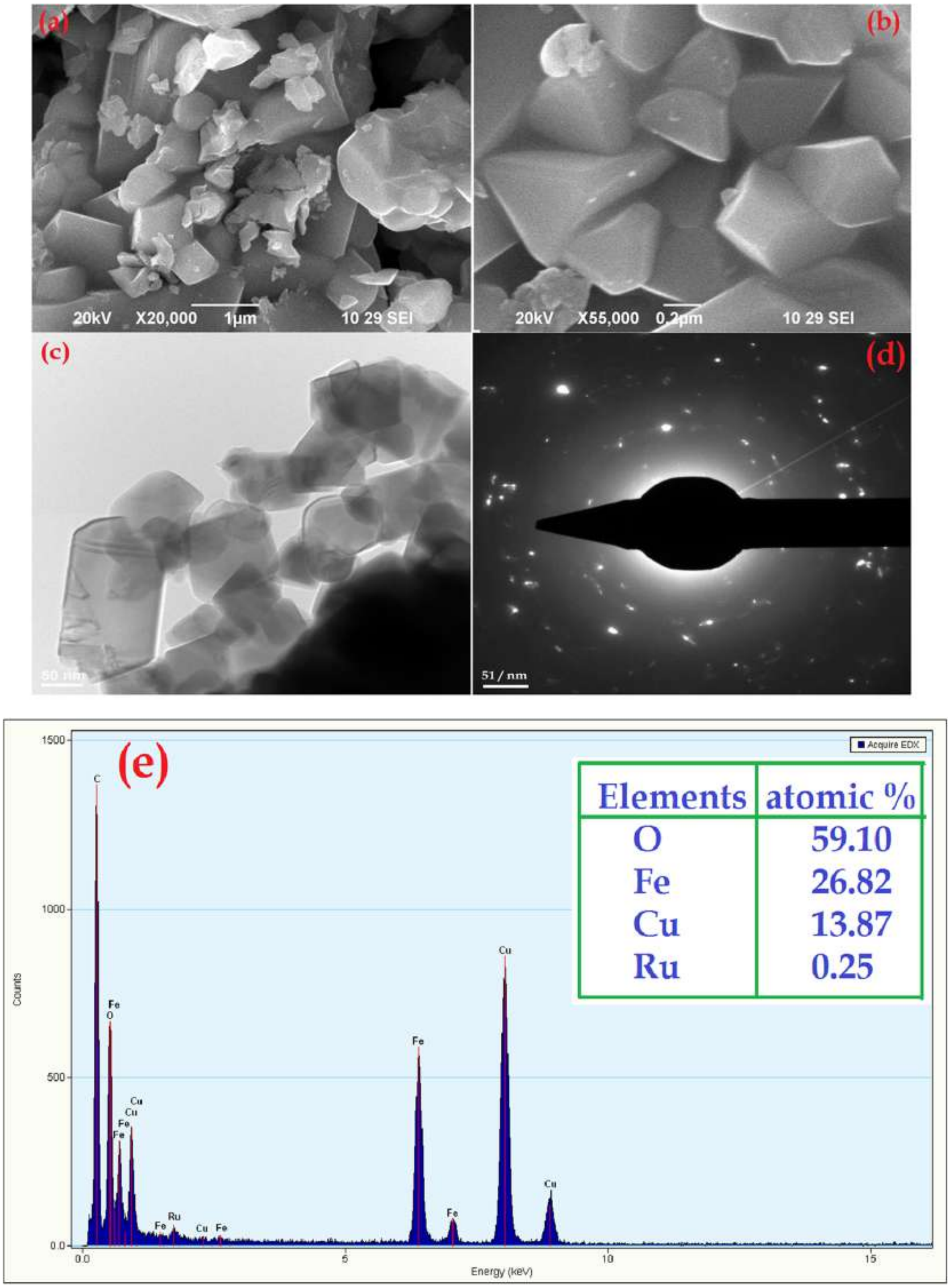

Fig. 2. (a-b) SEM, (c-d) TEM and (e) EDX images of Ru − $CuFe_2O_4$ NPs annealed at 900 °C.

this rate was slow, which is one of the common features of the ferrites [25–27]. The rise and down behaviors of dielectric constant were explained in accordance to Maxwell-Debye theory and interfacial or space charge polarization. The dielectric structure of Ru − $CuFe_2O_4$NPs could have two conducting layers; grains of higher conductivity and insulating grain boundaries [28]. Under the influence of applied field, motion of the charges could interrupt at the grain boundaries which are responsible for charge accumulation at the interface for interfacial or space charge polarization. The number of electrons transferred among Fe^{2+} and Fe^{3+} ions could be high at low frequencies which increases the space charge polarization as well as the dielectric constant. Also, the electron transferred among Fe^{2+} and Fe^{3+} ions couldn't follow the jumping frequency or high frequency, decreasing the space charge polarization and dielectric constant [28]. Apparently, the dielectric constant increased with annealing temperature which eventually increases the grain size, making easier for electrons to transfer for generating high contact between adjacent grains. Besides, the formation of Fe^{2+} ions increased at elevated annealing temperatures owing to Ru,

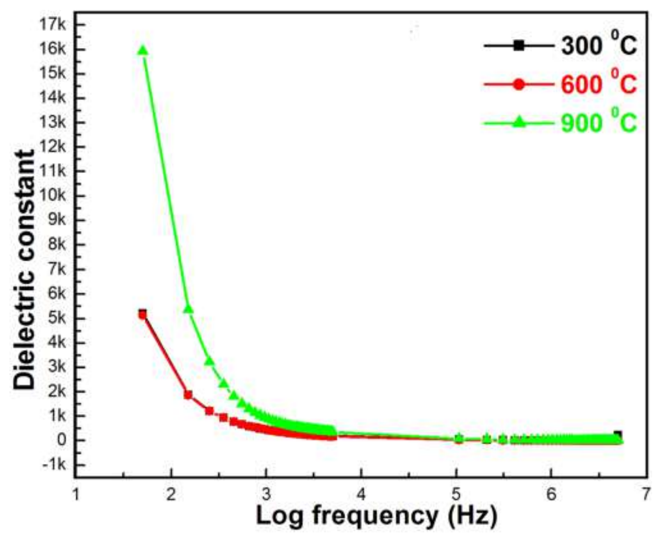

Fig. 3. Variations in dielectric constant of Ru − $CuFe_2O_4$ NPs annealed at different temperatures.

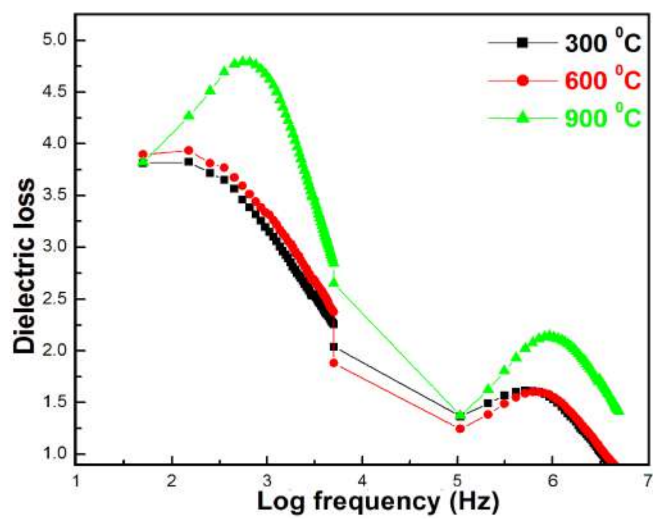

Fig. 4. Variations in dielectric loss of Ru − $CuFe_2O_4$NPs annealed at different temperatures.

Table 1
Structural, electrical and magnetic parameters of Ru − $CuFe_2O_4$ MNPs.

Parameters	$Ru_xCuFe_{2-x}O_4$ ($Ru_{0.02}Cu_1Fe_{1.98}O_4$)		
Temperature (°C)	300	600	900
Particle size (nm)	6.07	14.10	24.50
Dielectric constant	235.95	236.42	557.69
Dielectric loss	198.51	206.62	278.50
Coercivity (G)	744.12	166.59	366.50
Remanence (emu/g)	0.22	1.09	10.41
Saturation (emu/g)	1.39	6.81	21.88
Squareness ratio (M_r/M_s)	0.15	0.16	0.47

resulting in high polarization [25]. Therefore, the dielectric polarization increased *via* elevated annealing temperatures i.e. 300, 600 and 900 °C (Fig. 4). The jumping frequency of electron transfer among Fe^{2+} and Fe^{3+} ions could be equal to the frequency of applied field, the resonance peak was found in all samples [29]. The Fe ions might attain an equilibrium positions at A and B with equal potential energy, separated by a certain potential barrier. These ions could be transferred from A to B and B to A with equal probability. An alternative electric field applied with same frequency which transfers a maximum energy to ions, resulting in resonance peak in accordance to Debye relaxation theory. Also, the resonance peak observed at high frequencies [30,31]. The dielectric loss increased with increase of annealing temperatures owing to the less complicated motion of free charges at elevated temperatures. Another reason for dielectric loss could be a lag of polarization due to involvements of impurities and crystal imperfections. Basically, the dielectric properties are composition, density, grain size, microstructure, homogeneity and impurities dependent [32]. From Table 1, the Ru − $CuFe_2O_4$ NPs have proven to be a low dielectric loss, suggesting their suitability in high frequency devices [33].

3.4. Magnetic properties

Room-temperature hysteresis loops of Ru − $CuFe_2O_4$ NPs obtained at 300, 600 and 900 °C temperatures are shown in Fig. 5 with a low coercivity, saturation and remanence magnetization, suggesting Ru − $CuFe_2O_4$ NPs hold the soft magnetic character. The magnetizations increased with annealing temperatures. The magnetic ion distribution could change in the $CuFe_2O_4$where the tetrahedral and octahedral sites hold the equal number of Fe^{3+} ions with Ru^{3+} ions located at tetrahedral sites which minimizes the magnetic moment at tetrahedral sites and resulting the increased magnetization [34]. Also, the crystalline phase decides the magnetization. Here, the Ru − $CuFe_2O_4$ NPs were cubic in crystal structure thereby, their presence at larger unit cell volume as compared to tetragonal structure may also be one of the factor in increase of magnetization [35]. The particle size increased in accordance to the annealing temperature, enhancing the magnetic collinearity, soft magnetic nature and magnetization on deducing the spin canting effect [35]. Moreover, an improved crystallinity resulted an enhanced magnetic domain alignment [36]. Therefore, the magnetization could sufficiently be strong due to doping and re-distribution of sublattices in presence of non-magnetic Ru^{3+} ions [37]. As the magnetic moment of Fe^{3+} ions was greater over Ru^{3+} which can also be one of the factors for increased magnetization [38]. From Table 1, the variation in the magnetic parameters as a function of annealing temperatures was attributable to increase of the particle size. Likewise, cation redistribution plays a vital role in the saturation magnetization. With addition of Ru ions or non-magnetic ions partially replace the Fe^{3+} ions from tetrahedral sites could be responsible for an expected slightly increase of the saturation magnetization. Because of the exchange coupling among Fe^{3+} ions and Ru^{3+} ions, the saturation magnetization values increased with annealing temperature [39]. Contrarily, decreased coercivity on rising the annealing temperature directly related to the particle size which eventually increases with annealing temperature due to a process of re-crystallization. Remanence magnetization was elevated from 0.22 to 10.41 emu/g with annealing temperature, suggesting the rise of anisotropic properties of the Ru − $CuFe_2O_4$ NPs [36]. Under high annealing temperatures, squareness ratio increased from 0.15 to 0.47, depicting the generation of soft magnetic characteristics in the Ru − $CuFe_2O_4$NPs [3]. From table 1, the calculated squareness ratio was less than 0.50, demonstrating an involvement of single-domain crystals with uniaxial anisotropy even though the Ru − $CuFe_2O_4$ NPs was in cubic in structure [40–42].

4. Conclusion

This report deals with soft wet chemical synthesis and enhanced magnetization incubicFd3mspacegroupedRu − $CuFe_2O_4$ NPs whose crystallite size increases from 6 to 24 nm. The SEM and TEM images have corroborated well-defined cuboids. Dielectric properties are tuned with air-annealing temperatures. Also, values of dielectric constant and

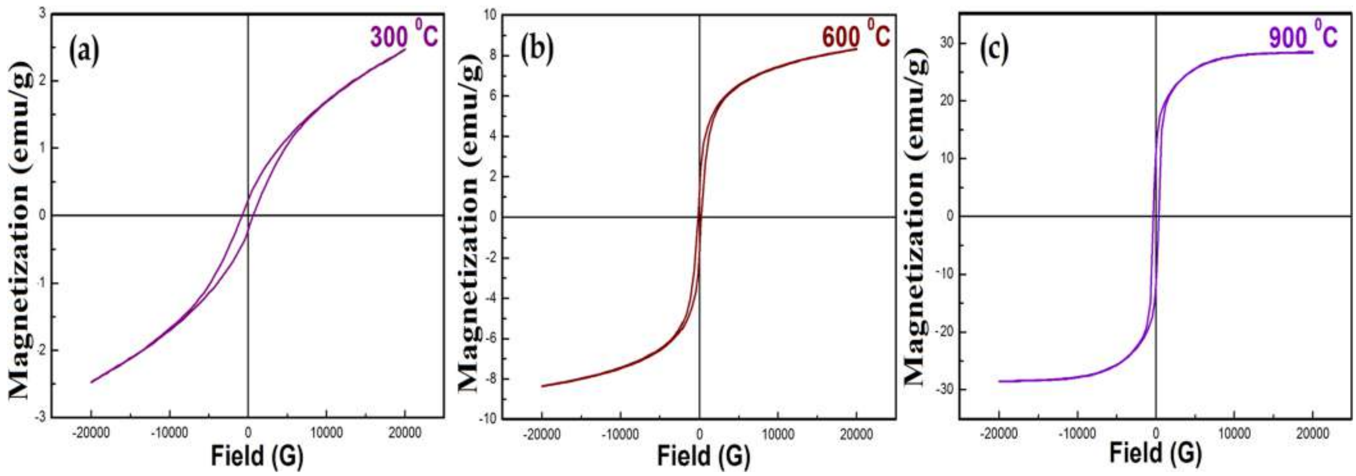

Fig. 5. Magnetic behaviour of $Ru - CuFe_2O_4$ NPs annealed at different temperatures.

loss are reduced with annealing temperatures. Soft magnetic nature has been approved in the hysteresis loop of $Ru - CuFe_2O_4$ which increases with an annealing temperature.

Appendix A. Supplementary data

Supplementary data to this article can be found online at https://doi.org/10.1016/j.jmmm.2018.12.050.

References

[1] C. Liu, B. Zou, A.J. Rondinone, Z.J. Zhang, Reverse micelle synthesis and characterization of superparamagnetic $MnFe_2O_4$ spinel ferrite, Nanocrystallites 104 (2000) 5–9, https://doi.org/10.1021/jp993552g.

[2] W. Zhong Lv, B. Liu, Z. Kuan Luo, X. Zhong Ren, P. Xin Zhang, XRD studies on the nanosized copper ferrite powders synthesized by sonochemical method, J. Alloys Compd. 465 (2008) 261–264, https://doi.org/10.1016/j.jallcom.2007.10.049.

[3] G.F. Goya, H.R. Rechenberg, J.Z. Jiang, Structural and magnetic properties of ball milled copper ferrite, J. Appl. Phys. 84 (1998) 1101, https://doi.org/10.1063/1.368109.

[4] M.M. Rashad, R.M. Mohamed, M.A. Ibrahim, L.F.M. Ismail, E.A. Abdel-Aal, Magnetic and catalytic properties of cubic copper ferrite nanopowders synthesized from secondary resources, Adv. Powder Technol. 23 (2012) 315–323, https://doi.org/10.1016/j.apt.2011.04.005.

[5] M. Sultan, R. Singh, Magnetization and crystal structure of RF-sputtered nanocrystalline $CuFe_2O_4$ thin films, Mater. Lett. 63 (2009) 1764–1766, https://doi.org/10.1016/j.matlet.2009.05.027.

[6] S. Krupička, P. Novák, Oxide spinels, Handb. Ferromagn. Mater. 3 (1982) 189–304, https://doi.org/10.1016/S1574-9304(05)80090-2.

[7] S. Krupička, P. Novák, K.T. Jacob, C.B. Alcock, The oxygen potential of the systems $Fe + FeCr_2O_4 + Cr_2O_3$ and $Fe + FeV_2O_4 + V_2O_3$ in the temperature range 750–1600°C, Metall. Trans. B. 3 (1975) 215–221, https://doi.org/10.1007/BF02913562.

[8] V. Manikandan, A. Vanitha, E. Ranjith Kumar, J. Chandrasekaran, Effect of in substitution on structural, dielectric and magnetic properties of $CuFe_2O_4$ nanoparticles, J. Magn. Magn. Mater. (2017), https://doi.org/10.1016/j.jmmm.2017.02.030.

[9] V.S. Yadav, K. Sahu, V.S. Yadav, D.K. Sahu, Y. Singh, M. Kumar, Frequency and temperature dependence of dielectric properties of pure Poly Vinylidene Fluoride (PVDF) thin films, AIP Conf. Proc. 267 (2010), https://doi.org/10.1063/1.3510553.

[10] R.K. Selvan, C.O. Augustin, L.J. Berchmans, R. Saraswathi, Combustion synthesis of $CuFe_2O_4$, Mater. Res. Bull. 38 (2003) 41–54, https://doi.org/10.1016/S0025-5408(02)01004-8.

[11] M.J. Iqbal, N. Yaqub, B. Sepiol, B. Ismail, A study of the influence of crystallite size on the electrical and magnetic properties of $CuFe_2O_4$, Mater. Res. Bull. 46 (2011) 1837–1842, https://doi.org/10.1016/j.materresbull.2011.07.036.

[12] H.M. Zaki, S.F. Mansour, The influence of Ge4+ and Ti4+ ions substitution on the magnetic properties of copper ferrite, Mater. Chem. Phys. 88 (2004) 326–332, https://doi.org/10.1016/j.matchemphys.2004.07.021.

[13] R. Zhang, Q. Yuan, R. Ma, X. Liu, C. Gao, M. Liu, C.L. Jia, H. Wang, Tuning conductivity and magnetism of $CuFe_2O_4$Via cation redistribution, RSC Adv. 7 (2017) 21926–21932, https://doi.org/10.1039/c7ra01765k.

[14] F. Caddeo, D. Loche, M.F. Casula, A. Corrias, Evidence of a cubic iron sub-lattice in t-$CuFe_2O_4$ demonstrated by X-ray absorption fine structure, Sci. Rep. 8 (2018) 797, https://doi.org/10.1038/s41598-017-19045-8.

[15] C. Singh, S. Bindra Narang, I.S. Hudiara, Y. Bai, F. Tabatabaei, Static magnetic properties of Co and Ru substituted Ba-Sr ferrite, Mater. Res. Bull. 43 (2008) 176–184, https://doi.org/10.1016/j.materresbull.2007.06.050.

[16] A.A. Sattar, A.H. Wafik, K.M. El-Shokrofy, M.M. El-Tabby, Magnetic properties of Cu-Zn ferrites doped with rare earth oxides, Phys. Status Solidi Appl. Res. 171 (1999) 563–569, https://doi.org/10.1002/(SICI)1521-396X(199902)171:2<563::AID-PSSA563>3.0.CO;2-K.

[17] S.E. Shirsath, R.H. Kadam, S.M. Patange, M.L. Mane, A. Ghasemi, A. Morisako, Enhanced magnetic properties of Dy $^{3+}$ substituted Ni-Cu-Zn ferrite nanoparticles, Appl. Phys. Lett. 100 (2012) 42407, https://doi.org/10.1063/1.3679688.

[18] Orn Helgason, Jean-Marc Greneche, Frank J. Berry, Frederick Mosselmans, The influence of ruthenium on the magnetic properties of γ-Fe_2O_3 (maghemite) studied by Mossbauer spectroscopy, J. Phys.: Condens. Matter 15 (2003) 2907.

[19] V. Manikandan, A. Vanitha, E. Ranjith Kumar, J. Chandrasekaran, Effect of sintering temperature on structural and dielectric properties of Sn substituted $CuFe_2O_4$ Nanoparticles, J. Magn. Magn. Mater. 423 (2017) 250–255, https://doi.org/10.1016/j.jmmm.2016.09.077.

[20] D. Maiti, U. Manju, S. Velaga, P.S. Devi, Phase evolution and growth of iron oxide nanoparticles: effect of hydrazine addition during sonication, Cryst. Growth Des. 13 (2013) 3637–3644, https://doi.org/10.1021/cg400627c.

[21] V. Manikandan, X. Li, R.S. Mane, Room temperature gas sensing properties of Sn-substituted nickel ferrite (NiFe2O4) thin film sensors prepared by chemical co-precipitation method, J. Electr. Mater. (2018) 2–7, https://doi.org/10.1007/s11664-018-6295-5.

[22] S.E. Shirsath, M.L. Mane, Y. Yasukawa, X. Liu, A. Morisako, Self-ignited high temperature synthesis and enhanced super-exchange interactions of Ho^{3+}–Mn^{2+}–Fe^{3+}–O^{2-} ferromagnetic nanoparticl, Phys. Chem. Chem. Phys. 16 (2014) 2347–2357, https://doi.org/10.1039/C3CP54257B.

[23] V. Manikandan, A. Vanitha, E. Ranjith Kumar, S. Kavita, Influence of sintering temperature on structural, dielectric and magnetic properties of Li substituted CuFe2O4 nanoparticles, J. Magn. Magn Mater. (2016), https://doi.org/10.1016/j.jmmm.2016.11.034.

[24] V. Manikandan, A. Vanitha, E. Ranjith Kumar, J. Chandrasekaran, Effect of sintering temperature on structural and dielectric properties of Sn substituted $CuFe_2O_4$ Nanoparticles, J. Magn. Magn. Mater. 423 (2017), https://doi.org/10.1016/j.jmmm.2016.09.077.

[25] C. Venkataraju, G. Sathishkumar, K. Sivakumar, Effect of nickel on the electrical properties of nanostructured MnZn ferrite, J. Alloys Compd. 498 (2010) 203–206, https://doi.org/10.1016/j.jallcom.2010.03.160.

[26] D.R.K. Latha, K. Satya Mohan, Dielectric behaviour of mixed Mn-Zn ferrites, Phys. Status Solidi Appl. Res. 142 (1994) K103–K106.

[27] S. Ramana, K.B. Reddy, Low-frequency dielectric behaviour of lithium-zinc ferrites, Physica Status Solidi (a) 273 (1992) 273–278.

[28] T. Jahanbin, M. Hashim, K. Amin, Mantori, Comparative studies on the structure and electromagnetic properties of Ni-Zn ferrites prepared via co-precipitation and conventional ceramic processing routes, J. Magn. Magn. Mater. 322 (2010) 2684–2689, https://doi.org/10.1016/j.jmmm.2010.04.008.

[29] C.G. Koops, On the dispersion of resistivity and dielectric constant of some semi-conductors at audiofrequencies, Phys. Rev. 83 (1951) 121–124, https://doi.org/10.1103/PhysRev. 83.121.

[30] P. Mathur, A. Thakur, M. Singh, S. Hill, Impact of processing and polarization on $Ni_xMn_{0.4-x}Zn_{0.6}Fe_2O_4$ spinel ferrites, Int. J. Modern Phy. B 23 (2009) 2523–2533.

[31] J. Parashar, V.K. Saxena, D. Jyoti, K.B. Sharma Bhatnagar, Dielectric behaviour of Zn substituted Cu nano-ferrites, J. Magn. Magn. Mater 394 (2015) 105–110, https://doi.org/10.1016/j.jmmm.2015.06.044.

[32] N. Varalaxmi, K.V. Sivakumar, Structural and dielectric studies of magnesium substituted NiCuZn ferrites for microinductor applications, Mater. Sci. Eng. B Solid-State Mater. Adv. Technol. 184 (2014) 88–97, https://doi.org/10.1016/j.mseb.2014.01.003.

[33] S.S. Jadhav, S.E. Shirsath, B.G. Toksha, S.M. Patange, D.R. Shengule, K.M. Jadhav, T. Jahanbin, M. Hashim, K. Amin Mantori, C. Venkataraju, G. Sathishkumar,

K. Sivakumar, Effect of nickel on the electrical properties of nanostructured MnZn ferrite, J. Alloys Compd. 322 (2010) 203–206, https://doi.org/10.1016/j.jallcom.2010.03.160.
[34] T.M. Hammad, J.K. Salem, A.A. Amsha, N.K. Hejazy, Optical and magnetic characterizations of zinc substituted copper ferrite synthesized by a co-precipitation chemical method, J. Alloys Compd. 741 (2018) 123–130, https://doi.org/10.1016/j.jallcom.2018.01.123.
[35] Z.K. Heiba, A.M. Wahba, M.B. Mohamed, Structural analysis and magnetic properties of biphasic chromium-substituted copper ferrites, J. Mol. Struct. 1147 (2017) 668–675, https://doi.org/10.1016/j.molstruc.2017.07.003.
[36] S.I. El-Dek, Effect of annealing temperature on the magnetic properties of $CoFe_2O_4$ nanoparticles, Philos. Mag. Lett. 90 (2010) 233–240, https://doi.org/10.1080/09500831003630732.
[37] M.R. Anantharaman, S. Jagatheesan, K.A. Malini, S. Sindhu, A. Narayanasamy, C.N. Chinnasamy, J.P. Jacobs, S. Reijne, K. Seshan, R.H.H. Smits, H.H. Brongersma, On the magnetic properties of ultra-fine zinc ferrites, J. Magn. Magn. Mater. 189 (1998) 83–88, https://doi.org/10.1016/S0304-8853(98)00171-1.
[38] P.P. Hankare, K.R. Sanadi, R.S. Pandav, N.M. Patil, K.M. Garadkar, I.S. Mulla, Structural, electrical and magnetic properties of cadmium substituted copper ferrite by sol-gel method, J. Alloys Compd. 540 (2012) 290–296, https://doi.org/10.1016/j.jallcom.2012.06.018.
[39] A.T. Raghavender, N.H. Hong, M. Kurisu, Enhanced magnetization by doping aluminum in laser ablated copper ferrite thin films, J. Magn. Magn. Mater. 401 (2016) 914–917, https://doi.org/10.1016/j.jmmm.2015.10.116.
[40] Y. Slimani, H. Güngüneş, M. Nawaz, A. Manikandan, H.S. El Sayed, M.A. Almessiere, H. Sözeri, S.E. Shirsath, I. Ercan, A. Baykal, Magneto-optical and microstructural properties of spinel cubic copper ferrites with Li-Al co-substitution, Ceram. Int. (2018), https://doi.org/10.1016/j.ceramint.2018.05.028.
[41] E.C. Stoner, E.P. Wohlfarth, A mechanism of magnetic hysteresis in heterogeneous alloys, IEEE Trans. Magn. 27 (1991) 3475–3518, https://doi.org/10.1109/TMAG.1991.1183750.
[42] V. Manikandan, Juliano C. Denardin, S. Vigniselvan, R.S. Mane, Structural dielectric and enhanced soft magnetic properties of lithium (Li) substituted nickel ferrite (NiFe2O4) nanoparticles, J. Magn. Magn. Mater. 465 (2018) 634–639, https://doi.org/10.1016/j.jmmm.2018.06.059.